Time-resolved lasing action from single and coupled photonic crystal nanocavity array lasers emitting in the telecom band

Dirk Englund,[1,a] Hatice Altug,[2] and Jelena Vučković[1]
[1]*Department of Electrical Engineering, Stanford University, Stanford, California 94305, USA*
[2]*Department of Electrical and Computer Engineering, Boston University, Boston, Massachusetts 02215, USA*

(Received 20 December 2008; accepted 12 March 2009; published online 7 May 2009)

We measure the lasing dynamics of single and coupled photonic crystal nanocavity array lasers fabricated in the indium gallium arsenide phosphide material system. Under short optical excitation, single cavity lasers produce pulses as fast as 11 ps (full width at half maximum), while coupled cavity lasers show significantly longer lasing duration which is not explained by a simple rate equation model. A finite difference time domain simulation including carrier gain and diffusion suggests that asynchronous lasing across the nanocavity array extends the laser's pulse duration.
 [DOI: 10.1063/1.3116563]

I. INTRODUCTION

The ultrasmall mode volume and high quality factor Q of cavities in photonic crystals (PCs) enable controllable light-matter interaction. This control can improve the performance of lasers by simultaneously increasing the spontaneous emission rate into the cavity mode while suppressing emission into all other modes, resulting in a large spontaneous emission coupling efficiency β.[1–5] Nanocavity lasers moreover enable very broad modulation bandwidth as the relaxation oscillation can be shifted beyond the cavity cutoff frequency.[6] We recently demonstrated single and coupled PC nanocavity array lasers in GaAs membranes with InGaAs quantum wells (QWs), emitting at 940–980 nm with a pulse duration of 7 ps [full width at half maximum (FWHM)] at low temperature[7] and a pulse duration shorter than 4 ps at room temperature.[8] There has been particular interest in PC lasers emitting in the transparency window of standard telecommunication fiber near 1550 nm.[9–11] We have recently addressed this wavelength band with PC nanocavity array lasers in the InGaAsP material system, emitting from 1530–1550 nm in quasicontinuous mode operation.[12] To increase power output from single cavities, we also described a coupled PC nanocavity array design. Here, we investigate the time-domain lasing characteristics of such coupled and single cavity PC lasers in the InGaAsP material system, to better understand their lasing dynamics and potential modulation rates. Under optical excitation with 3 ps pulses above the semiconductor's bandgap energy, we measure lasing response as fast as 11 ps for the single cavity structures. This is explained by a three-level rate equation model. However, the coupled cavity array laser has a longer response time, as long as 25 ps; this is not explained by the rate equation model. We instead analyze the coupled cavity array lasers with a finite difference time domain (FDTD) simulation incorporating a carrier gain model, which suggests that the extended lasing action results from spatially nonuniform optical pumping of nanocavities and results in asynchronous lasing action near threshold.

II. EXPERIMENT

The structures are fabricated in a 280 nm thick $In_{0.786}Ga_{0.214}As_{0.445}P_{0.555}$ membrane containing four 9 nm thick $In_{0.78}Ga_{0.22}As_{0.737}P_{0.263}$ QWs, separated by 20 nm barriers, as described in Ref. 13. The membrane rests on an InP substrate. PCs are created using electron beam lithography followed by a combination of wet and dry etching. We fabricated single cavities [Fig. 4(c)] and coupled cavity arrays [Fig. 1(a)] in square lattice PCs with periodicity $a=500$ nm and hole radii ranging from 160 to 230 nm. The array contains 9×9 cavities that are spaced by two holes. It supports a coupled quadrupole mode [Fig. 1(c)] that is designed to overlap with the QW gain.

The structures were tested in a confocal microscope setup at room temperature. The QWs were excited by pumping with a pulsed Ti:sapphire laser at an 80 MHz repetition rate with a pulse duration of 3.5 ps and a center wavelength of 770 nm, above the bandgap energy of the $In_{0.786}Ga_{0.214}As_{0.445}P_{0.555}$ membrane. The emission was measured using an optical spectrum analyzer and a streak camera (Hamatsu N5716-02) for time-resolved measurements.

The lasing response of a typical single cavity structure behavior is shown in the light-in/light-out (LL) curve in Fig.

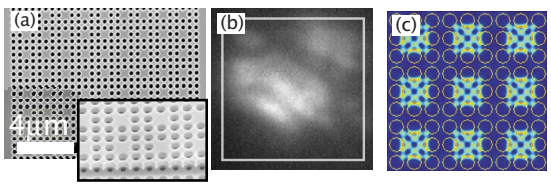

FIG. 1. (Color online) (a) Scanning electron micrograph of coupled nanocavity PC array. The inset shows the cross section of the PC membrane. (b) Far-field radiation pattern of coupled cavity array mode obtained at a pump power 1.4 above threshold. (c) Electric field intensity of coupled quadrupole mode.

[a]Electronic address: englund@fas.harvard.edu. Now at Harvard University, Departments of Physics and Chemistry.

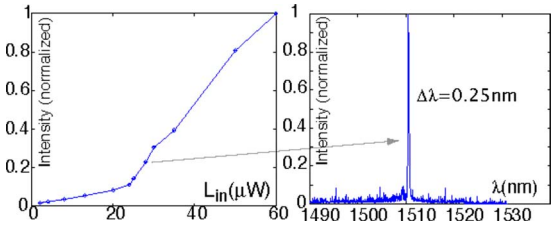

FIG. 2. (Color online) (a) LL curve of single cavity structure under pulsed excitation. (b) Single cavity laser spectrum at 28 μW averaged pump power.

2(a) and indicates a threshold of $\langle L_{in}\rangle = 22\ \mu$W time-averaged power (corresponding to ~71 mW peak power in a 3.5 ps pulse). At an average pump power of $\langle L_{in}\rangle = 28\ \mu$W, we observe a lasing mode with a FWHM of 0.25 nm at 1511 nm [Fig. 2(b)]. A streak-camera measurement at 30 μW indicates a lasing response with FWHM of ~11 ps. This is shown in Fig. 3(a). We analyze the lasing dynamics using the rate equation model described in Ref. 14. Briefly, this model assumes a homogeneous distribution of carriers across the spatial extent of the PC structure. The carriers are considered to be either in the ground, the pump, or in the lasing level. Using parameters derived from experiment, together with literature values for the gain and transparency carrier concentration,[15] the model predicts a cavity photon number $P'_{fit}(t)$. To compare $P_{fit}(t)$ with the experiment, we first convolve it with the streak-camera response function (modeled as a Gaussian pulse with FWHM=3 ps). The resulting cavity photon number $P_{fit}(t)$ is in good agreement with the experimental data in Fig. 3(a).

To estimate the maximum modulation rate of the single cavity laser, we excited the structure with a series of pulses produced with an etalon setup in the excitation path. A small angle misalignment in the etalon caused consecutive pulses to walk off from the excitation path, so that only two pulses are visible in the streak-camera measurement of the pump [center panel of Fig. 3(c)]. The laser is pumped at 1.4 times above the threshold, where it showed stable operation. The pulse separation shown is 21 ps and represents the smallest

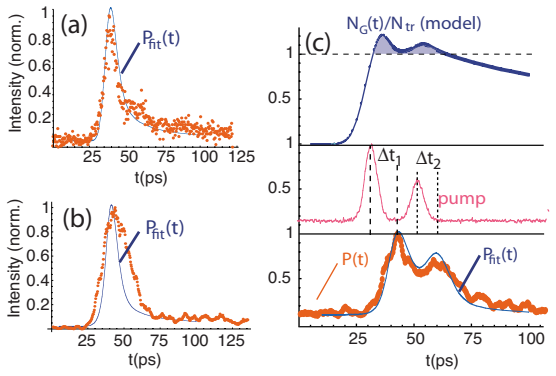

FIG. 3. (Color online) (a) Single cavity lasing response (dots) and rate equations fit P_{fit}. Pump power $\langle L_{in}\rangle = 31\ \mu$W. All plots are normalized to the maximum intensity. (b) Coupled-cavity array lasing response ($\langle L_{in}\rangle = 1.4$ times threshold). The rate equations model do not adequately explain the long lasing duration. The delay between pump and lasing action equals Δt_1 (Δt_2) for the first (second) pulse. (c) Single cavity response to excitation by two pulses: top, lasing level concentration; center, measured excitation sequence; bottom, observed intensity and rate equations fit.

pulse separation that resulted in two clearly distinguishable lasing response pulses [bottom panel of Fig. 3(c)]. This pulse repetition is longer than the sub-10 ps repetition time reported for single-cavity photonic crystal lasers in GaAs membranes with InGaAs QWs.[8] The laser turn-on delay is $\tau_1 = 11$ ps for the first pulse and $\tau_2 = 9$ ps for the second pulse. To understand the lasing dynamics, we again model the system with the rate equation model. The result is shown in the solid curve $P_{fit}(t)$ and fits the data well. It is useful to consider the lasing level concentration $N_G(t)$ predicted by the model; it is plotted in the top panel of Fig. 3(c), normalized by the carrier transparency concentration $N_{tr} \sim 1.5 \times 10^{18}$ cm^{-3}. The fraction of carriers that exceeds the transparency value (shaded region) is efficiently converted to cavity photons during the lasing process, since the threshold carrier concentration roughly equals the transparency concentration; the remainder recombines primarily through nonradiative recombination at the PC hole boundaries, with a recombination time given by $\tau_{nr} = r/2S$, where r and S are the hole radius and the surface recombination velocity, respectively.[16,17] This decay is also visible in the spontaneous emission tail in the bottom panel of Fig. 3(c). From separate lifetime measurements, we estimate $\tau_{nr} \approx 270$ ps, which gives $S \approx 3 \times 10^4$ cm/s. This value is two to three times higher than the value of $S \sim 10^4$ cm/s reported elsewhere for this material system,[12,18] probably due to the processing of the holes. The slower decay of carriers that remain after the first lasing pulse [roughly equal to N_{tr} in the top panel of Fig. 3(c)] strongly impacts the dynamics of the second laser pulse and would lead to eye-closing under a pseudorandom bit sequence. Therefore, return-to-zero signaling would be problematic at a modulation rate exceeding $\sim 1/\tau_{NR}$ unless the laser is pumped far above threshold where the remaining carrier concentration N_{tr} becomes insignificant. In our suspended structures, thermal problems made it difficult to achieve stable lasing action above ~1.6 times the threshold power. Heat dissipation can be improved by fabricating the PC laser structures on top of low-index substrates such as sapphire or silicon oxide.[10,11,19–21]

We next turn to the 9×9 PC nanocavity array. At a pump power of two times above threshold and below, we measured significantly longer lasing duration. For a pump intensity of 1.4 times above threshold, where we achieved stable operation, we measured FWHM ≈ 19 ps [Fig. 3(b)]. This longer response time is not adequately explained by the rate equations model, as shown in the poor match of the best fit to the data.

III. DISCUSSION

We believe that the poor fit to the rate equations model arises in large part because it does not account for spatial variations in the carrier concentration across the PC device. It was found previously that the spatial profile significantly impacts lasing dynamics, for example, through spatial hole burning,[22] and is important in understanding lasing threshold.[17] To understand its role in the laser time response, we have implemented a model of the carrier dynamics in our FDTD simulation. Such nonlinear FDTD implementations

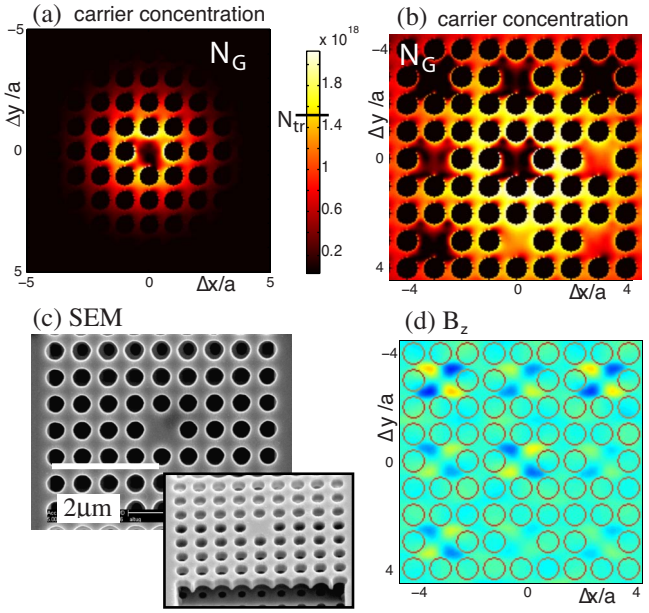

FIG. 4. (Color online) (a) Lasing-level carrier concentration (1 ps after injection) showing density gradient toward lasing cavity. Spatial hole burning results from the fast stimulated recombination during the lasing pulse. Pump power is $2\times N_{tr}$ at the center of the Gaussian spot with radius $2a$, where a is the PC lattice period. (b) Carrier concentration in PC array, 1 ps after injection. Pump energy corresponds to $1.4\times N_{tr}$. Small inhomogeneities in the pump spot (radius $6a$) and coupled cavity mode can result in a spreading of lasing onset times, contributing to longer total pulse duration. (c) Scanning electron micrograph (SEM) of single cavity InP laser structure. (d) Out-of-plane magnetic field of lasing mode, 1 ps after carrier injection.

have been used previously to model the dynamics in PC lasers.[23] Material gain is implemented in FDTD by an effective conductivity σ, as in Refs. 24 and 25. An auxiliary differential equation is used to describe the evolution of the current density $\vec{J}$. In turn, $\vec{J}$ is related to the carrier density N_G (assumed here to be equal for holes and electrons). The set of equations obtained when $\vec{J}=\sigma\vec{E}$ is substituted into Maxwell's equations is then expressed in the time domain and discretized as described in Ref. 23.

A simulation of optical pumping with a spatially Gaussian-shaped beam results in inhomogeneous gain and asynchronous lasing action, spreading out the total pulse duration. This is seen from the lasing level concentration N_G and cavity field in Figs. 4(b) and 4(d), recorded here 1 ps after injecting carriers at 1.4 times the transparency concentration in the center. The cavities are in different stages of the lasing cycle: in some cavities, the gain has already been used up [dark cavities in (b)], while other cavities are still at the onset of lasing [bright cavities in (b)]. The corresponding cavity fields are shown in the B_z component of the field in (d). The carrier concentration in (b) is blurred through carrier diffusion with an ambipolar diffusion constant of 7 cm^2/s.[26] As a result of the asynchronous lasing action across the coupled-cavity array, the nanocavities are not phase locked together, and the total response time is broadened. This hypothesis is supported by the microscope image in Fig. 1(b), which shows that the laser emission at 1.4 times threshold is not uniform across the structure. Experimentally it appears that at higher pump power, the pulse response becomes shorter; unfortunately, the lasing response becomes unstable when the pump power exceeds roughly 1.4 times the threshold power, so we were not able to acquire reliable data on the streak camera. Nevertheless, this observation is supported by our nonlinear FDTD model, as all cavities would reach lasing threshold more rapidly.

IV. SUMMARY

In conclusion, we have measured time-resolved lasing action of single and coupled nanocavity lasers in the InGaAsP/InP material system and emitting near the telecommunication band. Single cavity lasers show a lasing response as fast as 11 ps (FWHM) at 1.5 times above the threshold power, but their modulation rate appears approximately two times slower than that of InGaAs/GaAs PC lasers, probably due to slower nonradiative recombination. The significantly longer response time of the coupled cavity array structure indicates that under excitation with short pulses, it is difficult to excite the full PC structure uniformly to achieve phase locking across all nanocavities. This result suggests that large-signal modulation of the coupled cavity array laser requires attention to uniform injection current.

ACKNOWLEDGMENTS

This work was supported by the MARCO Interconnect Focus Center and the NSF. D.E. was supported by an NSF fellowship.

[1] M. Fujita, S. Takahashi, Y. Tanaka, T. Asano, and S. Noda, Science **308**, 1296 (2005).
[2] D. Englund, D. Fattal, E. Waks, G. Solomon, B. Zhang, T. Nakaoka, Y. Arakawa, Y. Yamamoto, and J. Vučković, Phys. Rev. Lett. **95**, 013904 (2005).
[3] S. Strauf, K. Hennessy, M. T. Rakher, Y.-S. Choi, A. Badolato, L. C. Andreani, E. L. Hu, P. M. Petroff, and D. Bouwmeester, Phys. Rev. Lett. **96**, 127404 (2006).
[4] S. Noda, M. Fujita, and T. Asano, Nat. Photonics **1**, 449 (2007).
[5] K. Nozaki, S. Kita, and T. Baba, Opt. Express **15**, 7506 (2007).
[6] G. Bjork and Y. Yamamoto, IEEE J. Quantum Electron. **27**, 2386 (1991).
[7] H. Altug, D. Englund, and J. Vučković, Nat. Phys. **2**, 484 (2006).
[8] D. Englund, H. Altug, I. Fushman, and J. Vučković, Appl. Phys. Lett. **91**, 071126 (2007).
[9] O. Painter, R. K. Lee, A. Scherer, A. Yariv, J. D. O'Brien, P. D. Dapkus, and I. Kim, Science **284**, 1819 (1999).
[10] J.-K. Hwang, H.-Y. Ryu, D.-S. Song, I.-Y. Han, H.-W. Song, H.-K. Park, Y.-H. Lee, and D.-H. Jang, Appl. Phys. Lett. **76**, 2982 (2000).
[11] C. Monat, C. Seassal, X. Letartre, P. Viktorovitch, P. Regreny, M. Gendry, P. Rojo-Romeo, G. Hollinger, E. Jalaguier, S. Pocas, and B. Aspar, Electron. Lett. **37**, 764 (2001).
[12] H. Altug and J. Vučković, Opt. Express **13**, 8819 (2005).
[13] H. Altug, "Physics and applications of photonic crystal nanocavities," Ph.D. thesis, Stanford University, 2006.
[14] D. Englund, H. Altug, B. Ellis, and J. Vuckovic, Laser Photonics Rev. **2**, 1863 (2008).
[15] Gain is modeled as $g(n_G)=\Gamma g_0 v_g \ln(n_G/V_a N_{tr})$, with $V_a=\Gamma V_{mode}$ the active material volume, $\Gamma\approx 0.159$ the gain confinement factor, $V_{mode}=0.55N_{cav}(\lambda/n)^3$ the mode volume of N_{cav} cavities, $g_0\approx 1500/cm$, $v_g=c/n_{eff}$ the group velocity, $n_{eff}=2.6$ the effective index (Ref. 27), and $N_{tr}\approx 1.5\times 10^{18}$ cm^{-3} (from Ref. 27).
[16] K. Tai, T. R. Hayes, S. L. McCall, and W. T. Tsang, Appl. Phys. Lett. **53**, 302 (1988).
[17] D. Englund, H. Altug, and J. Vučković, Appl. Phys. Lett. **91**, 071124 (2007).
[18] H. Ichikawa, K. Inoshita, and T. Baba, Appl. Phys. Lett. **78**, 2119 (2001).
[19] C. Monat, C. Seassal, X. Letartre, P. Regreny, M. Gendry, P. Rojo Romeo, P. Viktorovitch, M. Le Vassor d'Yerville, D. Cassagne, J. P. Albert, E.

Jalaguier, S. Pocas, and B. Aspar, J. Appl. Phys. **93**, 23 (2003).
[20]G. Vecchi, F. Raineri, I. Sagnes, A. Yacomotti, P. Monnier, T. J. Karle, K.-H. Lee, R. Braive, L. Le Gratiet, S. Guilet, G. Beaudoin, A. Taneau, S. Bouchoule, A. Levenson, and R. Raj, Opt. Express **15**, 7551 (2007).
[21]B. B. Bakir, C. Seassal, X. Letartre, P. Regreny, M. Gendry, P. Viktorovitch, M. Zussy, L. Di Cioccio, and J.-M. Fedeli, Opt. Express **14**, 9269 (2006).
[22]T. Baba, D. Sano, K. Nozaki, K. Inoshita, Y. Kuroki, and F. Koyama, Appl. Phys. Lett. **85**, 3989 (2004).
[23]W. H. Pernice, F. P. Payne, and D. F. Gallagher, Opt. Express **15**, 11433 (2007).
[24]M. Kretschmann and A. A. Maradudin, J. Opt. Soc. Am. B **21**, 150158 (2004).
[25]S. C. Hagness, R. M. Joseph, and A. Taflove, Radio Sci. **31**, 931941 (1996).
[26]D. Marshall, A. Miller, and C. C. Button, IEEE J. Quantum Electron. **36**, 1013 (2000).
[27]L. A. Coldren and S. W. Corzine, *Diode Lasers and Photonic Integrated Circuits* (Wiley, New York, 1995).